hep-th/0312039

BOUNDARY RIGIDITY AND HOLOGRAPHY

M. Porrati [a] *and R. Rabadan* [b]

[a] *Department of Physics, New York University*
4 Washington Pl., New York NY 10012, USA

[b] *School of Natural Sciences, Institute for Advanced Studies*
Olden Lane, Princeton NJ 08540, USA

Abstract

We review boundary rigidity theorems assessing that, under appropriate conditions, Riemannian manifolds with the same spectrum of boundary geodesics are isometric. We show how to apply these theorems to the problem of reconstructing a $d+1$ dimensional, negative curvature space-time from boundary data associated to two-point functions of high-dimension local operators in a conformal field theory. We also show simple, physically relevant examples of negative-curvature spaces that fail to satisfy in a subtle way some of the assumptions of rigidity theorems. In those examples, we explicitly show that the spectrum of boundary geodesics is not sufficient to reconstruct the metric in the bulk. We also survey other reconstruction procedures and comment on their possible implementation in the context of the holographic AdS/CFT duality.

e-mail: massimo.porrati@nyu.edu, rabadan@ias.edu

Contents

1 Introduction

The holographic principle [1] is a potentially revolutionary new paradigm in quantum gravity, since it gives up the idea that a fundamental description of physics is local. In place of locality, the principle states that the fundamental degrees of freedom that describe quantum gravity in a region of $d+1$-dimensional space-time, called "the bulk" hereafter, are located on an appropriate d-dimensional subspace, a "screen" located somewhere in that region. A proper definition of such holographic screen can be given also in cases where the bulk has no boundary [2]. What is generally unknown, instead, is the

physics of the degrees of freedom that live on that screen. In the case that the background bulk space-time is Anti de Sitter (AdS) space, much more can be said. In that case it has been conjectured that quantum gravity –or better string theory– on AdS_{d+1} space (times some compact manifold of dimension $9-d$) has a dual description in terms of a d-dimensional (local) conformal field theory (CFT) defined on the boundary M_d of AdS_{d+1} [3]. A comprehensive review of the evidence in support of that conjecture can be found in [4].

The relation between quantum gravity in AdS_{d+1} and the CFT on M_d is a duality, because when one description is perturbative, the other is strongly coupled. So, for instance, in the canonical case when the duality is between the Type IIB superstring on $AdS_5 \times S_5$ and N=4, $SU(N_c)$ super Yang-Mills in four dimensions, one can trust the low-energy supergravity approximation to the superstring in the large N_c limit, and only when the 't Hooft coupling constant of the N=4 theory, $g^2_{YM}N$ is large.

The fact that the two dual descriptions are never simultaneously weakly coupled makes it difficult to establish an explicit "dictionary" associating states to the quantum gravity in AdS to states of the dual conformal field theory. Consider in particular the case where the quantum gravity wave function is peaked around a given classical geometry. A natural question one can ask is how to reconstruct this geometry from CFT boundary data only. This question does not have as yet a complete answer, even though much progress has been made in the last few years. For instance, proposals exist for the CFT description of precursors [5], and for how to detect, through CFT correlators, the region behind the horizon of an AdS black hole [6].

In this paper, we continue the program of "holographic" reconstruction of space-time by looking at a special class of CFT observables, namely the two-point correlators of local operators with high conformal dimension. We will investigate to what extent they can determine the geometry of the bulk space-time. The Green's functions we select are particularly simple because they are directly related to the geodesic distance of two boundary points in the (regularized) bulk space-time.

The reconstruction of the bulk space-time from boundary data reduces, in this approximation, to a classical problem in mathematics: the boundary rigidity problem. Its precise definition will be given in Section 2, here we can formulate it as follows: *under what conditions are two spaces with the same spectrum of geodesics, whose endpoints lie on the boundary, isometric?*

In Section 2, we will review the argument of ref. [7] connecting Green's functions to geodesic distance, and we will summarize existing theorems about boundary rigidity, paying particular attention to the assumption necessary to prove them. We will use some of these known results to show, for instance, that a small deformation of (Euclidean) AdS space is boundary rigid in any dimension.

In Section 3, we will examine some specific examples of bulk space-times: point particles in AdS_3, their equal-time sections, the BTZ black hole [8], the RP^2 geon [9], and their Euclidean continuation. We will show that some of those spaces are *not* boundary rigid. The reason for that failure will be traced back to the violation of some of the most subtle assumptions needed in proving general boundary rigidity theorems. The examples of Section 3, the AdS_3 point particle in particular, are in some sense the flip side of the findings in ref. [7].

That reference used Green's functions of operators with high conformal weight as holographic probes. Among other things, it showed that they can detect the formation of AdS_3 black holes in the collision of two point particles. So, those simple observables are nevertheless able to detect physics behind the black-hole horizon. In Section 3, instead, we find that there exist situations where the bulk space-time has no horizons, yet its metric cannot be reconstructed from the spectrum of its boundary geodesics.

In Section 4, we survey, without any pretense of completeness, other holographic reconstruction procedures, and we discuss which of them could be implemented using the AdS/CFT duality, i.e. from knowledge of CFT data only.

Section 5 contains our conclusions, together with a conjecture about a possible extension of boundary rigidity theorems, and its relation to the holographic duality.

2 Green's Functions, Geodesics, and Boundary Rigidity Theorems

2.1 From Green's Functions to Geodesics

This subsection, included here for completeness, follows closely ref. [7].

Near the boundary, the metric of an asymptotically Anti de Sitter space is

$$ds^2 = \frac{L^2}{z^2}[dz^2 + g_{\mu\nu}(z,x)dx^\mu dx^\nu], \qquad \mu,\nu = 1,.,4, \qquad g_{\mu\nu}(z,x) = g^0_{\mu\nu}(x) + O(z^2). \quad (1)$$

All non-light-like geodesics ending on the boundary $z = 0$ have infinite length, so the space must be regularized by cutting off a small region near the boundary, specifically, by restricting $z \geq \epsilon$. The length ϵ has a holographic counterpart in the boundary CFT: it is the UV cutoff one needs to regularize the theory [10, 11, 12]. Let us denote the cutoff $d+1$ dimensional bulk with $\mathcal{M}^\epsilon_{d+1}$. In $\mathcal{M}^\epsilon_{d+1}$, geodesics have finite length. Moreover, in this space, the boundary-to-boundary Green's function of a free scalar field field of mass m is well defined. This Green's function, $G(x,y)$, with $x, y \in \partial\mathcal{M}^\epsilon_{d+1}$, is interpreted as the (regularized) two-point function of some scalar composite operator in the dual CFT. The conformal dimension of the operator, Δ, is (generically) the largest root of the

equation

$$L^2 m^2 = \Delta(\Delta - d). \tag{2}$$

For large mass $mL \gg 1$, $\Delta = mL + d/2 + O(1/mL) \approx mL$. The Green's function of a free scalar field in AdS can be also represented as a functional integral

$$G(x,y) = \int [dX(t)] \exp(-\Delta D[X]/L), \tag{3}$$

where $D[X]$ is the length of the path $X(t)$ joining x to y. When $mL \gg 1$, the path integral is dominated by its saddle point, i.e. the boundary-to-boundary geodesic joining x to y:

$$G(x,y) = \text{const}\,\{1 + O[L/\Delta D_{min}(x,y)]\} \exp[-\Delta D_{min}(x,y)/L]. \tag{4}$$

Notice that in Eq. (4) we are ignoring inverse powers of the distance, so, even when more than one geodesic can be drawn between the points x, y, we should only take into account the contribution of the shortest one. To include the others would be inconsistent with our approximation [1]. In summary, we have found that the holographic correspondence and known results about the semi-classical approximation to free-field Green's functions relate, by Eq. (4), a CFT quantity (the two-point function of an operator of dimension $\Delta \gg 1$) to a geometrical quantity: the minimal geodesic distance between the two points.

2.2 Boundary Rigidity Theorems

Assume that a direct problem is well behaved, i.e. that its solution exists, is unique, stable etc. The inverse problem is to extract some properties of the original object or system from the solution of the direct problem. These problems in general are ill-posed (in the sense of Hadamard): there may be no solution, or the solution may be non-unique, or unstable (small changes in the input data may result in large changes in the solution). Examples of inverse problems include inverse scattering (how to reconstruct the shape of a target, or a potential from the scattered field at large distances), the inverse gravimetry problem, tomography, inverse conductivity problems, inverse seismic problems, many problems in inverse spectral geometry & c.

Consider in particular a Riemannian manifold $(\mathcal{M}, g)$ with a boundary. Let $D_{min}(x,y)$ be the geodesic distance between two points at the boundary $x, y \in \partial\mathcal{M}$[2]. The function $D_{min}(x,y)$ is called the hodograph (a term borrowed from geophysics). The inverse problem is to find to what extent the Riemannian manifold is determined by the lengths of the geodesics between points at the boundary. Equivalently, the question is: up to what extent do the two-point functions in the conformal theory determine the bulk metric?

[1] Attempts to go beyond this limitation will be discussed in Sections 4 and 5.

[2] See reference [14] for a survey.

Solutions to this problem come into sets, related by diffeomorphisms that reduce to the identity at the boundary. That, of course, changes the metric in the interior, while keeping the same geodesic spectrum. A manifold is said boundary rigid if there exists only one such set of solutions.

Boundary rigidity theorems analyze the uniqueness of the solution. They give the conditions that a Riemannian manifold must satisfy to be boundary rigid, i.e. to be completely determined by the hodograph. If we take a manifold where there exist interior points that cannot be reached by any geodesic, then one can always change the metric close to this point without changing the length spectrum. So, general Riemannian manifolds are not boundary rigid. What are the conditions that a manifold should satisfy to be boundary rigid? One of the most natural conditions is that the manifold is simple; namely, its boundary is strictly convex, and every two points at the boundary are joined by a unique geodesic. Such a manifold is diffeomorphic to a ball. R. Michel conjectured in 1981 [15] that every simple manifold is rigid. Another natural condition considered by Croke [16] is that the manifold is strongly geodesic minimizing. This means that every segment of a geodesic that lies on the interior of the manifold is strongly minimizing, i.e. it is the unique path. The length spectrum determines the volume of the manifold for both simple and strongly geodesic minimizing manifolds.

The problem is not solved in general, but there are some partial results that will be useful to us. Simple Riemannian manifolds with negative curvature (like AdS) are deformation boundary rigid [17], i.e. we cannot deform the metric keeping the boundary distance fixed. This result was generalized [18] and further in [20] for compact dissipative Riemannian manifolds (convex boundary plus a condition on the maximal geodesics) satisfying some inequality concerning the curvature. There is a semi-global result in [19] when one of the metrics is close to the Euclidean and the other satisfies a bound on the curvature.

For general metrics, not just deformations, a theorem exists in two dimensions [22]: every strong geodesic minimizing manifold with non-positive curvature is boundary rigid. This theorem has been recently generalized to subdomains of simple manifolds in two dimensions [21]. Any compact sub-domain with smooth boundary of any dimension in a constant curvature space (Euclidean space, hyperbolic space or the open hemisphere of a round sphere) is boundary rigid [15, 23, 24]. Apart from that spaces and sub-domains of negatively curved symmetric spaces and some products of spaces[3] there are no other boundary rigid examples.

The Lorentzian case has not been analyzed very much. The two dimensional case is analyzed in ref. [25], which tries to extend the result of Croke [22] to the Lorentzian case. The condition analogous to being strong geodesically maximizing is not enough to

[3]See the survey [14].

guarantee that the manifold is boundary rigid.

3 Examples and "Counterexamples"

3.1 Point Particle in AdS_3

The metric for a point particle in AdS_3 is locally the same as AdS_3, but with different global identifications. It reads

$$ds^2 = \frac{1}{r^2+\gamma^2}dr^2 - (r^2+\gamma^2)dt^2 + r^2 d\phi^2, \qquad r \geq 0, \qquad 0 \leq \phi < 2\pi. \tag{5}$$

By redefining $r = \gamma\hat{r}$, $\hat{t} = \gamma t$, $\hat{\phi} = \gamma\phi$, this metric can be recast in a standard AdS_3 form, but with a different periodicity for the $\hat{\phi}$ coordinate: $0 \leq \hat{\phi} < 2\pi\gamma$. This implies of course $0 \leq \gamma^2 < 1$. Negative γ^2 gives the non-rotating BTZ black hole metric.

To correctly analyze the geodesic between any two points at the boundary one has to consider the Euclidean version of the problem. In the Lorentzian version the problem is ill defined. The problems associated with Lorentzian signature (there are no geodesics between some points at the boundary, or an infinite number of them with the same length & c) can already be found in simple examples as AdS. In this section we will be mainly concerned with Euclidean metrics. Next we will study Euclidean AdS_3 with a point particle in three cases: at infinite temperature, where one studies its constant time section (which is the same as in the Lorentzian problem), at zero temperature, and finally at finite, nonzero temperature. We will find that, in some cases, non-rigidity appears.

3.1.1 Constant Time Section

Consider now the $t = 0$ section of this metric. Its geodesics can be easily found, e.g. using the Hamilton-Jacobi method. A standard calculation gives the angular distance between the boundary endpoints of the geodesic, $\Delta\phi$, as a function of its minimum distance from the center, $\bar{r}$:

$$\Delta\phi = \frac{1}{\gamma}\theta, \qquad \cot\theta = \frac{\bar{r}^2 - \gamma^2}{2\gamma\bar{r}}. \tag{6}$$

(Here we chose $\gamma > 0$). By definition, $0 \leq \theta < \pi$. In this range, Eq. (6) is one-to-one. This does not mean that there is only one geodesic joining any two boundary points! Indeed, when the angular distance $\Delta\phi$ is in the range $\pi < \Delta\phi < \pi/\gamma$, we have a second geodesic joining the same two boundary points, with $\Delta\phi' = 2\pi - \Delta\phi < \Delta\phi$. Since Eq. (6) is one-to-one, this means that the minimum radii of the two geodesics are different, hence the geodesics are distinct.

So, even if our space is "almost" AdS_3, and its sectional curvature is negative, this space may not be boundary rigid, since it fails to satisfy the simplicity condition. Moreover, it is singular at $r = 0$; removing the point $r = 0$ makes the space non-simply connected, so, again, non-simple.

If we were given the lengths of *all* geodesics between boundary points, it would be still far from obvious that the point-particle space could be deformed without changing *some* geodesic lengths. In our case, though, more than one geodesics can be drawn between the same two points, so we have to be careful about the identification of physically meaningful holographic data.

As we mentioned in Subsection 2.1, the physical quantities one is given in the boundary theory are the two-point function of composite operators. Geodesic are used to obtain a saddle point approximation of these functions. Since the saddle point approximation neglects inverse powers of the geodesic distance [see Eq. (4)], one should also neglect contributions from sub-dominant saddle points. So, the physical data are the lengths of *minimal* geodesics in between boundary points. Generically speaking, the minimal geodesic spectrum is not enough to reconstruct the bulk metric from boundary data. In our case, one can be more specific, and prove that there exist deformations of the metric that do not change the spectrum of minimal length geodesics. So, not only the conditions for boundary rigidity are not met in our simple example, but we can explicitly show that the bulk metric can be changed without affecting boundary data.

To see this, notice that the shortest geodesic is that for which $\Delta\phi < \pi$. This means that no minimal-length geodesic can come closer to the center than

$$r_{min} = \min_{0\leq\theta\leq\gamma\pi} \bar{r} = \gamma\sqrt{\frac{1-\cos(\gamma\pi/2)}{1+\cos(\gamma\pi/2)}}. \tag{7}$$

So, any change of the metric confined to the region $r < r_{min}$ is undetectable, within our approximation.

Now, let us ask whether it is possible to smooth out the singularity at $r = 0$ without changing the spectrum of minimum-length geodesics. This would mean that holography could be blind to qualitative features of the bulk space geometry, such as the very existence of singularities. It is convenient to change coordinates in Eq. (5) by setting $r = \gamma \sinh\rho$, and write the metric at $t = 0$ as

$$ds^2 = d\rho^2 + \gamma^2 \sinh^2\rho d\phi^2, \qquad \rho > 0. \tag{8}$$

Eq. (7) implies that the minimum distance ρ_{min} probed by minimal-length geodesics obeys $\gamma \sinh\rho_{min} < 1$. Now the question is, can we smooth out the metric by changing only the region $\rho < \rho_{min}$, while preserving some basic characteristics of the metric, for instance, that the curvature is negative? The answer is *no*. To see this, consider the

change $\gamma \sinh \rho \to F(\rho) \geq 0$. The new range of the coordinate ρ is from ρ_0, the point where F vanishes, to $+\infty$. Smoothness at ρ_0 requires $(dF/d\rho)|_{\rho_0} = 1$. To leave the metric outside ρ_{min} unchanged, we must also require $(dF/d\rho)|_{\rho_{min}} = \gamma \cosh \rho_{min}$

To keep the curvature negative, we must have $d^2F/d\rho^2 > 0$, whence the inequality

$$(dF/d\rho)|_{\rho_{min}} - (dF/d\rho)|_{\rho_0} = \gamma \cosh \rho_{min} - 1 = \int_{\rho_0}^{\rho_{min}} \frac{d^2F}{d\rho^2} d\rho > 0. \tag{9}$$

By using the value of $r_{min} = \gamma \sinh \rho_{min}$ given in Eq. (7), we finally find that, in order to smooth out the singularity without changing the geodesic spectrum, we must have

$$\gamma \cosh \rho_{min} = \gamma \sqrt{\frac{2}{1 + \cos(\gamma \pi/2)}} > 1. \tag{10}$$

This equation is never satisfied in the range $0 < \gamma < 1$.

So we have seen that there is no metric preserving rotational invariance that coincide with the point particle metric in the region accessible by geodesics and that has negative curvature. That means that all the metrics with this hodograph have positive curvature in some region so the theorems about dispersive manifolds with negative curvature (ref. [17] e.g.) do not apply. We can extend this proof for general deformations of the metric by considering the integral

$$k(\Sigma) = \frac{1}{4\pi} \int_\Sigma \mathcal{R}, \tag{11}$$

where Σ is a region in the interior of the Euclidean section of the space. On a compact manifold without boundary, k is the Euler number. In two dimensions the scalar-curvature density is a total derivative.

In our case, the curvature has two contributions: one from the point particle (a delta function at its position) and one from the AdS space itself. The first contribution to the number k can be expressed in terms of the deficit angle $\delta = 2\pi(1 - \gamma)$

$$k_{part}(\Sigma) = \frac{1}{2\pi} \delta. \tag{12}$$

The AdS space has constant negative curvature $\mathcal{R} = -2/R^2$. So, the total contribution in a region that contains the point particle is:

$$k(\Sigma) = \frac{1}{2\pi} \delta - \frac{1}{2\pi R^2} Vol_\Sigma. \tag{13}$$

The metric Eq. (8) has $R = 1$, so the critical volume when $k = 0$ is:

$$Vol_c = R^2 \delta = 2\pi(1 - \gamma). \tag{14}$$

By Eq. (10), the volume of the ball B of radius r_{min} –i.e. the region not probed by minimal-length geodesics– is

$$V_B = 2\pi\gamma\left(\sqrt{\frac{2}{1+\cos(\gamma\pi/2)}}-1\right). \tag{15}$$

Can we change the metric within a region $\Sigma_0 \subset B$ to a *smooth*, negative-curvature one, without touching the outside metric? Again, the answer is no, since if this were possible, then, for that metric, $k(\Sigma_0) < 0$. On the other hand, for the AdS point-particle metric:

$$k(\Sigma_0) = (1-\gamma) - \frac{1}{2\pi R^2} Vol_\Sigma > (1-\gamma) - \gamma\left(\sqrt{\frac{2}{1+\cos(\gamma\pi/2)}}-1\right) > 0. \tag{16}$$

So we need $k(\Sigma_0)$ to be positive for a metric, and negative for another. This is impossible, because for any open region Σ, $k(\Sigma)$ is invariant under any change of the metric inside Σ, that reduces to the identity on its boundary, since the scalar curvature is a total derivative.

3.1.2 Finite and Zero Temperature AdS_3 with a Point Particle

Now let us consider the whole Euclidean AdS_3 with a point particle in it. It is easy to see that the shortest geodesic joining points separated by a very long Euclidean time can get arbitrarily close to the origin, as the time interval gets larger. Let us consider geodesics with only a time separation ($\Delta\phi = 0$). The trajectory satisfy the equation:

$$\frac{dr}{dt} = \frac{(\gamma^2+r^2)}{E}\sqrt{m^2(\gamma^2+r^2)-E^2}, \tag{17}$$

that can be integrated to:

$$t = \frac{\gamma}{2}\log\frac{\gamma\sqrt{m^2(\gamma^2+r^2)-E^2}+Er}{\gamma\sqrt{m^2(\gamma^2+r^2)-E^2}-Er}, \tag{18}$$

where E and m are the energy and the mass of the particle.

Starting at the boundary there is a family of solutions with $|E^2| > |m^2|\gamma^2$ that do not touch the origin (see figure 1). The geodesics start from the boundary and go back at $\Delta\phi = 0$. The time to come back is:

$$\Delta T = \gamma\log\frac{E+m\gamma}{E-m\gamma}. \tag{19}$$

Notice that for $|E^2| \to |m^2|\gamma^2$ the time interval diverges. That means that they can be arbitrarily long, and joining any two points on the boundary. The turning point is at

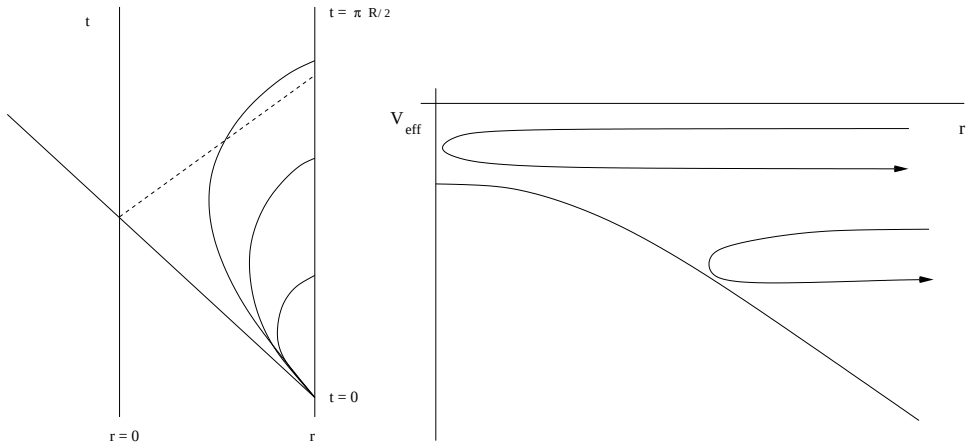

Figure 1: Left: geodesics without angular momentum in Euclidean AdS_3. Right: effective potential for particles in Euclidean AdS_3 without angular momentum.

$r_c^2 = E^2/m^2 - \gamma^2$. For $|E^2| \leq |m^2|\gamma^2$ the geodesics pass through the origin and reach the antipodal point $\Delta\phi = \pi$. But, as we have seen from the constant time sections, these are not shortest geodesics.

So in the whole AdS_3 with a point particle the shortest geodesics cover the whole space (except the point where the point particle is located) due to long time geodesics.

The finite temperature case can be obtained by imposing the periodicity conditions $t \to t + \beta$. In this case the shortest geodesics cannot cover the whole space, as there is a maximum to the time difference $\Delta T = \beta/2$. So, there is a region close to the point particle that cannot be reached by the shortest geodesics: the higher the temperature the larger the region. Notice that one needs both a point particle in the AdS space and finite temperature to have manifest non-rigidity.

3.2 Lorentzian BTZ Black Hole

3.2.1 Description of the Space

One can represent the non-rotating BTZ black hole as an orbifold of AdS_3 by a boost [4]. To define the action of the boost, let us define AdS_3 as a hyperboloid in a flat space of signature $(+,+.-,-)$: $x_0^2 + x_1^2 - x_2^2 - x_3^2 = 1$. The boost action is:

$$x_1 \pm x_2 \to e^{\pm 2\pi r_+}(x_1 \pm x_2). \tag{20}$$

[4] In this subsection we will follow references [8, 6, 32].

There is a line of singularities at the fixed points of the boost $x_1 = x_2 = 0$. Near the singularity, the metric reduces to that of a Milne universe times a line.

Let us decompose AdS_3 into three regions, each of which is further subdivided into four others, classified by a pair of signs $\eta_{1,2} = \pm$:

- Region 1: $x_1^2 - x_2^2 \geq 0$, $x_0^2 - x_3^2 \leq 0$,

$$\begin{aligned} x_1 \pm x_2 &= \eta_1 \frac{r}{r_+} e^{\pm r_+ \phi} \\ x_3 \pm x_0 &= \eta_2 \frac{\sqrt{r^2 - r_+^2}}{r_+} e^{\pm r_+ t}. \end{aligned} \tag{21}$$

- Region 2: $x_1^2 - x_2^2 \geq 0$, $x_0^2 - x_3^2 \geq 0$,

$$\begin{aligned} x_1 \pm x_2 &= \eta_1 \frac{r}{r_+} e^{\pm r_+ \phi} \\ x_3 \pm x_0 &= \eta_2 \frac{\sqrt{r_+^2 - r^2}}{r_+} e^{\pm r_+ t}. \end{aligned} \tag{22}$$

- Region 3: $x_1^2 - x_2^2 \leq 0$, $x_0^2 - x_3^2 \geq 0$,

$$\begin{aligned} x_1 \pm x_2 &= \eta_1 \frac{\sqrt{r^2 - r_+^2}}{r_+} e^{\pm r_+ t} \\ x_3 \pm x_0 &= \eta_2 \frac{r}{r_+} e^{\pm r_+ \phi}. \end{aligned} \tag{23}$$

Notice that regions 1 and 3 reach the boundary at $r \to \infty$, while in region 2 the radial variable ranges from 0 to r_+. The singularity, located at the fixed points of the orbifold action, is at $r = 0$, i.e. in region 2.

The boost identifies ϕ with $\phi + 2\pi$ in regions 1 and 2, and $t \to t + 2\pi$ in region 3.

The metric in these new coordinates is:

$$ds^2 = -(r^2 - r_+^2)dt^2 + \frac{dr^2}{(r^2 - r_+^2)} + r^2 d\phi^2, \tag{24}$$

then, the coordinate t is timelike in regions 1 and 3, and spacelike in region 2. That gives closed timelike curves in region 3. To go from region 2 to region 3 we have to pass very close to the singularity. We will try to find results that are independent of the eventual resolution of the singularity in the final, complete theory of quantum gravity, so, we will not study geodesics that come close to it, and consider only regions 1 and 2.

The boundary is made of a set of disconnected patches labeled by the region where they belong: $1_{(\eta_1,\eta_2)}$ and $3_{(\eta_1,\eta_2)}$.

3.2.2 Boundary Geodesics

Let us take a spacelike geodesic starting at the boundary of region 1_{++}. To begin with, we do not want to consider geodesics that get infinitely close to the singularity. Then, we have to restrict ourselves to geodesics ending at the boundary of 1_{++} (that do not cross the horizon) or at the boundary of 1_{+-} (that cross the horizon).

We use the Hamilton-Jacobi method to obtain the time and angular difference between the two points at the boundary in function of the energy and angular momentum:

$$\Delta t = 2\int_{r_c}^{\infty} \frac{dr}{N(r)^2} \frac{E}{\sqrt{E^2 - V(r)^2}}, \tag{25}$$

and

$$\Delta\phi = 2\int_{r_c}^{\infty} dr \frac{l}{r^2} \frac{1}{\sqrt{E^2 - V(r)^2}}, \tag{26}$$

where $N(r)^2 = r^2 - r_+^2$ and $V(r)^2 = N(r)^2(l^2/r^2 - 1)$ is the effective potential.

The above integrals can be explicitly solved by

$$\Delta\phi = \frac{1}{r_+} \log\left(\frac{(E^2 - (l + r_+)^2)r_c^2}{r_c^2(E^2 - l^2 - r_+^2) + 2r_+^2 l^2}\right), \tag{27}$$

and

$$\Delta T = \frac{1}{r_+} \log\left(\frac{4r_+^2 l^2 - (E^2 - l^2 - r_+^2)^2 + (E^2 - l^2 + r_+^2)\sqrt{\Delta}}{2(r_c^2 - r_+^2)(2Er_+ + E^2 - l^2 + r_+^2)}\right), \tag{28}$$

where $r_c^2 = \frac{1}{2}(l^2 + r_+^2 - E^2 + \sqrt{\Delta})$ is the positive root of $E = V(r)$ and $\Delta = (l^2 + r_+^2 - E^2)^2 - 4r_+^2 l^2$.

For energies $0 < E^2 < (l - r_+)^2$ the particle does not reach the singularity and is reflected to the boundary. For larger energies, $E^2 > (l - r_+)^2$, the particle crosses the horizon and reaches the singularity. To stay away from the singularity, we will restrict to energies $0 < E^2 < (l - r_+)^2$. In this range of energies, we have two possible behaviors: some geodesics are reflected back to the boundary of region 1_{++} (if $r_+ < l$), while other geodesics cross the horizon and reach the boundary of region 1_{+-} (if $l < r_+$) (see figure 2).

At $E = 0$, the particle arrives at the point $r = r_+$ (if $r_+ > l$) or $r = l$ (if $r_+ < l$). It never crosses the horizon. In the case $r_+ > l$ it reaches the other boundary, and it is reflected back when $r_+ < l$. When we increase the energy, while keeping l fixed, both ΔT and $\Delta\phi$ increase and become infinity when the energy reaches its maximum.

3.2.3 Geodesics Outside the Horizon

Let us consider first the case $r_+ < l$. One can get arbitrarily close to the horizon with geodesics both of whose ends belong to the boundary by taking $l \to r_+$ and $E \to 0$.

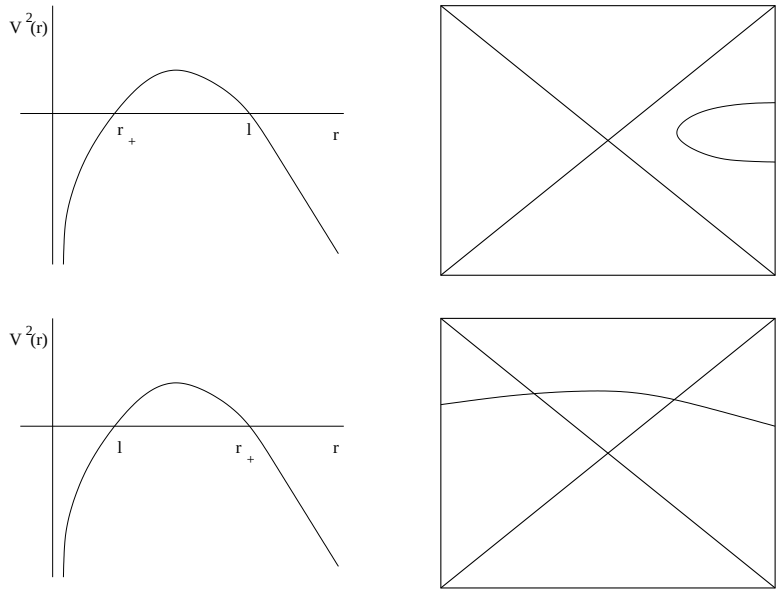

Figure 2: Potential and corresponding trajectories on the Poincaré diagram for trajectories that do not approach the singularity $[0 < E^2 < (l - r_+)^2]$. For $r_+ < l$, the geodesic does not reach the horizon and goes back to the boundary 1_{++} (upper left picture). For $r_+ > l$, the geodesic reaches the horizon and arrives at the boundary 1_{+-} (lower left picture).

In this limit $\Delta\phi$ diverges as we are getting close to the horizon. That means that the geodesics wind many times close to the horizon.

That can be easily seen for Euclidean sections, i.e $E = 0$, and for geodesics within the region 1_{++}. The angular variable can be expressed in terms of the angular momentum

$$e^{r_+\Delta\phi} = \left(\frac{l + r_+}{l - r_+}\right)^2 . \tag{29}$$

The shortest geodesics can probe the space up to a minimum radius $r_c = r_+/\tanh(\pi r_+/4)$. Now, if we increase the energy, the geodesics with fixed angular difference are farther away from the horizon. This means that r_c is a boundary beyond which no shortest geodesic (with both ends at the same boundary) can penetrate.

Let us take the endpoints at $y_i = (t_i, r = 1/\epsilon, \phi_i)$ for very large r and let us assume that $(\Delta\phi + 2\pi n)^2 > (\Delta t)^2$ for all integers. Then, there exist infinitely many geodesics connecting these two points, labeled by an integer number n. The proper length of the geodesics is:

$$\sinh^2(L/2) = \frac{1}{\epsilon^2 r_+^2}\sinh^2[r_+(\Delta\phi)/2] - \left(\frac{1}{\epsilon^2 r_+^2} - 1\right)\sinh^2[r_+(\Delta t)/2]. \tag{30}$$

When the regulator ϵ is taken to zero we get:

$$\exp(L_n) = \frac{2}{\epsilon^2 r_+^2}\left[\cosh^2(r_+(\Delta\phi + 2\pi n)) - \sinh^2(r_+(\Delta t))\right]. \tag{31}$$

The behavior of these geodesics is easy to understand: they can wind several times close to the horizon. The closer they get to the horizon, the higher is their winding number n.

3.2.4 Geodesics Crossing the Horizon

Consider now the case when the particle crosses the horizon, i.e. $l < r_+$. Notice that by taking $T \to T + i\pi/r_+$ we pass from region 1_{++} to region 1_{+-}.

To illustrate how the geodesics behave, let us take $l = 0$. In both cases $\Delta\phi = 0$. By naively continuing the integrals we find:

$$r_+\Delta T = \log\left(\frac{|E^2 - r_+^2|}{(E + r_+)^2}\right) + \pi i. \tag{32}$$

This is interpreted as a geodesic going from region 1_{++} to region 1_{+-}.

Now, we can ask ourselves if for these geodesics there exists a region that cannot be explored by shortest geodesics (the first question here is what we mean by "shortest").

As the geodesics probe inside the horizon, that region has to lie in the interior of the horizon. Similarly to the case when geodesics end on the same boundary, we start with $E = 0$ ($\Delta T = 0$). The geodesic touches the horizon and reaches the other boundary. When we increase the energy for fixed angle, the angular momentum decreases (i.e. the orbit get closer to the center). To go very close to the singularity we have to take $l = 0$, that is the case just explained above.

3.3 Euclidean BTZ Black Hole

The metric of the Euclidean BTZ black hole is defined starting from the Lorentzian one by continuing to imaginary time:

$$ds^2 = (r^2 - r_+^2)d\tau^2 + \frac{dr^2}{(r^2 - r_+^2)} + r^2 d\phi^2, \tag{33}$$

where the radial variable goes from $r = r_+$ to infinity and the Euclidean time has period π/r_+ to avoid conical singularities at $r = r_+$. The boundary is a two dimensional torus parametrized by the Euclidean time and the angular variable. The interior is a solid 3-d torus, where the points $r = r_+$ form a circle at its center. The manifold is non simple, as there is more than one geodesic between any two points at the boundary (geodesics can wind). That is easy to see by considering the uncompactified version, obtained by taking the angular variable ϕ non periodic. This space is again the Euclidean AdS (that is best seen by defining a new variable $x^2 = r^2 - r_+^2$), and, as we know, this space is boundary rigid. Notice that this example can also be interpreted as AdS at finite temperature, where the same kind of reasoning applies. The temperature is identified with $T = r_+/\pi$.

The shortest geodesics reach every point at the interior. This is easily seen because the sections of constant ϕ are disks, were the shortest geodesics can connect every two points. This is a necessary but not sufficient condition for boundary rigidity. Whether the space is actually boundary rigid is a nontrivial question, which is answered in the affirmative if the conjecture in Section 5 is true.

3.4 The RP^2 Geon

The RP^2 geon [9] can be obtained from AdS_3 by quotienting by the action of a discrete group generated by:

$$x_1 \pm x_2 \to e^{\pm \pi r_+}(x_1 \pm x_2). \tag{34}$$

and $x_3 \to -x_3$. So, this space is the quotient of the BTZ black hole by a Z_2 symmetry.

In region 1 of the BTZ black hole, the geon corresponds to identifying under the transformation $\phi \to \phi + \pi$, $\eta_2 \to -\eta_2$ and $t \to -t$. That is, region 1_{++} is mapped into

region 1_{+-}, i.e. the two exterior regions of the BTZ black hole are interchanged. The geon is thus a black hole with a single exterior region, isometric to the region 1_{++} of the BTZ black hole. Spacelike hypersurfaces are quotients of a cylinder (parametrized by $x \sim r - r_+$ and ϕ) by a freely acting Z_2: $\phi \to \phi + \pi$ and $x \to -x$. Topologically, this is RP_2 minus the point at $r = \infty$.

In region 2, the action of the Z_2 group is the same as in region 1. In particular, it interchanges region 2_{++} with region 2_{+-}. The Penrose diagram is half of the Penrose diagram of the BTZ black hole, with the upper left part reflected into the lower right part, and the lower left part into the upper right one.

In region 1 of the BTZ black hole, the geon corresponds to identifying t with $t+\pi$, η_2 with $-\eta_2$, and ϕ with $-\phi$. As in the BTZ black hole, there exist closed timelike curves.

The geodesics ending at the boundary are as in the BTZ black hole, taking into account that the boundary of 1_{++} is equivalent to the boundary of region 1_{+-}. So, for every two points at the boundary, there are geodesics that cross the horizon.

3.5 Euclidean RP^2 Geon

To construct the Euclidean RP^2 geon one takes the Euclidean BTZ, and quotients it by a Z_2 symmetry: $\phi \to \phi + \pi$ and $t \to -t$. The sections at fixed radius are Klein bottles (the two dimensional torus with a Z_2 identifications). At the horizon, the Klein bottle degenerates to a circle.

The geodesics connecting points at the boundary can be easily computed by considering the Euclidean BTZ geodesics, and identifying the points at the boundary as above. The geodesics of the BTZ black hole can be obtained from the Euclidean AdS_3 ones by the identification $\phi \to \phi+2\pi$. Said in another way, the geodesics of the geon are the same as in AdS_3 when taking into into account the identification between boundary points: $\phi \to \phi + \pi$ and $t \to -t$.

Let us write the BTZ black hole metric in the form:

$$ds^2 = r^2 d\tau^2 + \frac{dr^2}{1+r^2} + (1+r^2)d\phi^2, \tag{35}$$

with periods $\tau \to \tau + 2\pi$ and $\phi \to \phi + 2\pi r_+$. To see if the shortest geodesics cover the whole space we have to compare the distance between two geodesics (see figure 3): the first one, that is also present in the BTZ, has $\Delta T = \pi$ and $\Delta\phi = 0$ [let us call it geodesic a, joining point $(\tau = \pi/2, \phi)$ to $(\tau = 3\pi/2, \phi)$]. The other one, that joins points identified by the Z_2 symmetry, has $\Delta T = 0$ and $\Delta\phi = \pi r_+$ [geodesic b, joining point $(\tau = \pi/2, \phi)$ to $(\tau = \pi/2, \phi + \pi r_+)$, that is the Z_2 image of $(\tau = 3\pi/2, \phi)$].

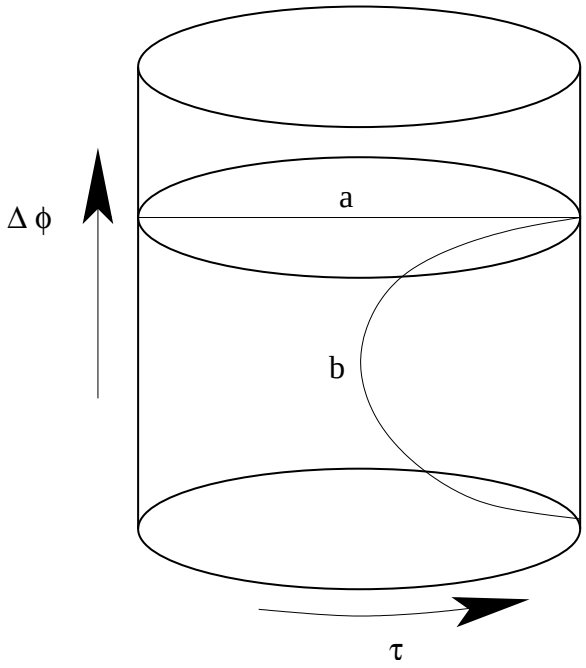

Figure 3: Two candidates for the shortest geodesic in the geon. Geodesics of type a cover the whole space, while geodesics of type b do not reach a portion of the space close to the horizon.

The difference in length of the two geodesics is:

$$l_a - l_b = \log\left[\frac{4e^{-\pi r_+}}{(1-e^{-\pi r_+})^2}\right]. \tag{36}$$

For small r_+ ($r_+ \ll 1$), the geodesic b is the shortest one. It never reaches the center. It is easy to see that in this case there is a region inside the geon that cannot be reached by any shortest geodesics.

For large r_+ ($r_+ \gg 1$), the geodesic a is the shortest. It lies on a constant ϕ section of the torus, and, as in the BTZ black hole, covers the whole space.

In the RP^2 case, one can construct a linear combination of two-point correlation functions that does not receive contributions from the shortest geodesic [9]. So, both geodesics a and b can be unambiguously determined by boundary data. Equivalently, in this case, the boundary data are the lengths of all geodesics that lift to minimal-length ones in the Z_2 cover of the RP^2 geon, that is the BTZ black hole. They do probe the entire space. So, while one cannot reconstruct the geon metric from the spectrum of shortest geodesics only, more refined boundary data may allow to establish a rigidity theorem.

3.6 Higher-Dimensional Finite-Temperature AdS Black Holes

Now, let us consider the higher-dimensional AdS Black Hole. In this case, there are two geometries contributing the boundary $S^1 \times S^{d-1}$: the AdS Schwarzschild Black Hole ($X_2 = R^2 \times S^{d-1}$) and AdS at finite temperature ($X_1 = S^1 \times R^d$). Unlike in dimension three, the Euclidean version of these spaces have different topology. In [35, 11], it has been shown that the dominant geometry at low temperatures is AdS at finite temperature, while at high temperature the dominant contribution is the black hole. As we have seen from the previous examples, constant-time geodesics in finite-temperature AdS cover the whole space, so we expect this space to be boundary rigid. At higher temperature, the dominant contribution comes from the black hole that, unlike in three dimension, is not boundary rigid. That can be seen using constant-angle geodesics (then the problem is reduced to a disk parametrized by time and the radial coordinate).

This is a very interesting case, since the same boundary admits two different geometric theories, one that is boundary rigid and other that is not. The different geometries have been identified in [11] with two different phases of the same boundary CFT.

Space	Description	Boundary Rigid	Non Boundary Rigid	Boundary Rigid Cover
Point Particle in AdS_3	Constant Time Section		X	N/A
	Zero Temperature	X		X
	Finite Temperature		X	X
BTZ Black Hole	AdS_3/Z	X		X
RP^2 Geon $r_+ \ll 1$	$AdS_3/Z_2 \otimes_S Z$		X	X
RP^2 Geon $r_+ \gg 1$	$AdS_3/Z_2 \otimes_S Z$	X		X
Finite Temperature AdS_d	AdS_d/Z	X		X
AdS_d Black Hole			X	N/A

Table 1: Summary table of the different examples analysed in this section.

4 Other Bulk Reconstruction Procedures

We have seen that the leading contribution of massive particle propagators reproduces a unique metric when the manifold is boundary rigid. We have seen several familiar examples of three dimensional manifolds that are boundary rigid and other manifolds that are not.

We may ask about other structures that can be obtained from the field theory that will tell us other information about the Riemannian manifold. Here we review other procedures that will allow us to partially reconstruct the interior Riemannian manifold.

4.1 Dirichlet-to-Neumann Map

Let $(\mathcal{M}, g)$ be a Riemannian manifold with boundary $\partial\mathcal{M}$, and consider the following problem: find the field ϕ such that $\Delta_g\phi = 0$ on $\mathcal{M}$ with a given boundary value $\phi|_{\partial\mathcal{M}} = J$, where J is a source at the boundary. The Dirichlet-to-Neumann map is the value of the normal derivative of the solution to the above problem at the boundary: $\partial_n\phi|_{\partial\mathcal{M}} = n^i\partial_i\phi|_{\partial\mathcal{M}}$. In this way we can define a unique function depending on the sources $\partial_n\phi|_{\partial\mathcal{M}}(J)$.

The map is directly related to field theory observables. In the AdS/CFT correspondence, the metric g has a double pole at the boundary $\partial\mathcal{M}$ [see Eq. (1)]. This requires that we regularize the manifold by cutting it off at finite proper distance from the boundary, $z = \epsilon$, as we did in Subsection 2.1. In the dual interpretation in terms of CFT data, $1/\epsilon$ is a UV cutoff of the field theory, needed to properly define composite operators. The field ϕ is dual to a CFT operator, O. When the linearized equation of motion of ϕ is $\Delta_g\phi = 0$, then the operator O has conformal dimension $\Delta = d = \dim\partial\mathcal{M}$. The field $\phi(z, x)$ can be expanded as [11, 12, 13]

$$\phi(\epsilon, x) = \phi_0(x) + \epsilon^2\phi_2(x) + ... + \epsilon^d \log\epsilon^2\phi_d(x) + \epsilon^d\psi_d(\epsilon, x). \tag{37}$$

The coefficients $\phi_2, ..\phi_d$ are *known, local* functions of $\phi_0(x)$ and $\psi_d(\epsilon, x) = \psi_d(0, x)+O(\epsilon^2)$. So, in Eq. (37) there are two unknown functions: $\phi_0(x)$ and $\psi_d(\epsilon, x)$. The Dirichlet-to-Neumann data allow to fix them both. In the limit $\epsilon \to 0$, $\phi_0(0)$ is identified with the source I of the the operator O, while $\psi_d(0, x)$ becomes proportional to the VEV of the operator O. More precisely [11, 12, 13],

$$\psi_d(0, x) = 4\langle 0|O(x)\exp\left(-\int_{\partial\mathcal{M}} IO\right)|0\rangle. \tag{38}$$

The inverse problem[5] consists in extracting information about the Riemannian manifold from the Dirichlet-to-Neumann map $\partial_n\phi|_{\partial\mathcal{M}}(J)$.

It is conjectured that the for manifolds of dimension $dim(\mathcal{M}) > 2$ the Dirichlet-to-Neumann map determines the Riemannian manifold uniquely (for dimension two it determines uniquely the conformal class of the metric). It has been proved by Uhlmann and collaborators [27, 28, 29, 30] that the Dirichlet-to-Neumann map determines the Riemannian metric for real-analytic manifolds of dimension $dim(\mathcal{M}) > 2$ and the conformal structure for C^∞ manifolds and $dim(\mathcal{M}) = 2$.

[5]This inverse problem has appeared in several fields. It was proposed by Calderon [22] in 1980, motivated by geophysical prospection. It also appears in Electrical Impedance Tomography (EIT) in trying to obtain the conductivity of a medium by making voltage and currents measurements on the boundary.

4.2 Scattering Relation

Imagine a geodesic that starts and ends at the boundary of a Riemannian manifold. The scattering relation is a function that, for a starting point and initial velocity of a geodesic at the boundary, gives the final point and the final velocity at the boundary: $\alpha(x_i, v_i) = (x_f, v_f)$. For that map to be well defined, we demand that the Riemannian manifold is non-trapping, i.e. that each maximal geodesic is finite. The scattering relation is an involution (α^2 is the identity).

In the dual field theory, one may think of obtaining this relation from a two-point correlator of a dimension-$\Delta \gg 1$ operator as follows.

The correlator of two (bare) operators in the regularized theory with cutoff ϵ is, thanks to Eq. (4),

$$\langle O(x)O(y)\rangle_\epsilon \propto \exp[-\Delta D_{min}(x,y)/L]. \tag{39}$$

We can convolute $\langle O(x)O(y)\rangle_\epsilon$ with a function $f(x)$, localized around x_i within an uncertainty δ:

$$\int_{\partial\mathcal{M}^\epsilon} f(x)\langle O(x)O(y)\rangle_\epsilon. \tag{40}$$

This function also localizes the momentum components along the boundary, $p = -i\partial/\partial x$, within an uncertainty $1/\delta$ around a central value p_i. In the geodesic approximation, the mass-shell condition $L^2\sum_{m=1}^{d+1} p_m p^m = \Delta(\Delta - d) = m^2L^2$ holds. So, we also know the normal component of the momentum, within an uncertainty $1/\delta$. Whenever $p_i \gg 1/\delta$, and the boundary is sufficiently smooth, we may reasonably approximate the result of the convolution by assigning an initial position x_i and initial velocity $v_i = p_i/m$ to the geodesic

$$\int_{\partial\mathcal{M}^\epsilon} f(x)\langle O(x)O(y)\rangle_\epsilon \approx \exp[-\Delta D_{v_i}(x_i, y)/L]. \tag{41}$$

Clearly, in this approximation, the two-point function is nonzero only for a specific value of y, to wit: the final point x_f. Eq. (41) also uniquely defines the final velocity v_f (by convoluting it with an approximate eigenstate of the final momentum) hence the scattering relation.

The problem with this procedure is that it does not give an exact dispersion relation, but only an approximate one. This is because Eq. (41) is exact only in the classical limit. Even within the semiclassical approximation, Eq. (41) is contaminated by extremal trajectories beginning near (x_i, v_i). To be concrete, imagine the case that two trajectories join the points x_i, x_f; one with initial velocity v_i, the other with initial velocity w_i. Both trajectories contribute to Eq. (41). To estimate the contribution of the second, denote by $\tilde{f}$ the Fourier transform of f. For f Gaussian of width δ we have, approximately,

$\tilde{f}(mv) \approx \exp[-\delta\Delta^2(v-v_i)^2/2L^2]$; so, Eq. (41) becomes, with obvious notations

$$\int_{\partial\mathcal{M}^\epsilon} f(x)\langle O(x)O(y)\rangle_\epsilon \approx \exp[-\Delta D_{v_i}(x_i,y)/L]+\exp[-\delta\Delta^2(w_i-v_i)^2/2L^2-\Delta D_{w_i}(x_i,y)/L]. \tag{42}$$

The second contribution can be neglected only if

$$\exp[-\delta\Delta^2(w_i-v_i)^2/2L^2 - \Delta D_{w_i}(x_i,y)/L + \Delta D_{v_i}(x_i,y)/L] \ll 1. \tag{43}$$

This restricts the validity of Eq. (41) to manfolds which, even though non-simple, do not have geodesics with lenght too close to the minimizing one. To make precise statements on non-minimizing geodesics, we need additional information on the CFT, as explained later in Subsection 4.4 and in the Conclusions.

The inverse problem is whether the scattering relation determines the metric. In the case that the manifold is simple the scattering relation is equivalent to the boundary distance function for the two points at the boundary [15]. It has been shown in [21] that in two dimensional simple manifolds the Dirichlet-to-Neumann map is determined by the scattering relation. So in this case the scattering relation, the hodograph and the Dirichlet-to-Neumann map are related.

4.3 Bulk to Boundary Functions

A complete information about the metric on the manifold is given by the bulk to boundary Green function for very massive fields. Again, in the limit of very high mass this function is very well approximated by the distance $r_x(y)$ between a point at the interior of the manifold $x \in \mathcal{M}$ and a point at the boundary $y \in \partial\mathcal{M}$. Now let us consider the function $\mathcal{R}$ that assigns to every point $x \in \mathcal{M}$ its boundary distance function $\mathcal{R} : x \in \mathcal{M} \to r_r \in L^\infty(\partial\mathcal{M})$, where $L^\infty(\partial\mathcal{M})$ is the space with the norm:

$$||r|| = sup_{z\in(\partial\mathcal{M})}|r(z)|. \tag{44}$$

Let us call $\mathcal{R}(\mathcal{M})$ the set of all boundary distance functions. In [31] it is shown that one can construct a differential structure and a metric on the set of the boundary distance functions such that it becomes isometric to the original Riemannian manifold.

To see how it works, let us consider first the case of geodesically regular manifolds (there is a unique geodesic between any two points in the bulk, and the geodesic goes to the boundary). Then we will consider the general case. Take two points x and x' in the interior of $\mathcal{M}$ and compute the function:

$$\begin{aligned} f : \partial\mathcal{M} &\to R^+, \\ y &\mapsto |r_x(y) - r_{x'}(y)|. \end{aligned} \tag{45}$$

Using the triangular inequality one can easily see that $d(x, x') \geq f(y)$ for all points y. If in addition the manifold is regular, there is a unique geodesic that joins the points x and x' and that goes till the boundary (let us call this point at the boundary y_c). At this point the inequality is saturated: $d(x, x') \geq f(y)$. As there is only one geodesic (regular manifold) that means that the distance between the two points is just the maximum of $f(y)$.

That is: we can read what is the distance between any two points inside from the bulk to boundary function.

A direct extension of this reasoning will be to consider the case when there are several geodesics between the points x and x' (i.e one is the shortest and the other wind around the manifold). Then there are several local maxima. The lower of these maxima is the distance (measured by the shortest geodesic). The only requirement is that the geodesics arrive to the boundary. The proof of how the metric is reconstructed from the bulk to boundary functions for general manifolds can be found in [31].

So, if we know the bulk-to-boundary distance, we can easily reconstruct the bulk metric. Unfortunately, the holographic interpretation of this quantity is rather mysterious. In specific theories, as $SU(N)$, N = 4 super Yang-Mills, one may be able to extract it from expectation values of, say, $\mathrm{Tr}\, F_{\mu\nu}F^{\mu\nu}$, computed on a one-instanton background [33, 34]. The actual implementation of this program on a generic manifold is still unclear to us.

4.4 Spectral Boundary Data

Now, let us consider a different type of data. They are obtained from a differential operator (it must be elliptic, so we must work in Euclidean space) of the form:

$$D = -\frac{1}{\sqrt{g}}\partial_i(\sqrt{g}g^{ij}\partial_j) + V \tag{46}$$

where V is an arbitrary functions on $\mathcal{M}$. This operator can be obtained from an action:

$$S = \int f\sqrt{g}\left[(\partial\phi)^2 + V\phi^2\right] \tag{47}$$

that can be interpreted as the action of a massive particle ϕ with a position-dependent "mass" $m^2 = V$. Notice that if we have a dimensional reduction of the form $\mathcal{M} \times \mathcal{M}'$ to $\mathcal{M}$ with a warped metric, the warp factor can always be interpreted as a modification of the potential.

Now, let us consider the Dirichlet problem on $\mathcal{M}$, i.e. $\phi|_{\partial\mathcal{M}} = 0$. The boundary spectral data is the collection of all the eigenvalues λ_k and the normal derivatives of the eigenfunctions at the boundary $\partial_n\phi_k|_{\partial\mathcal{M}} = n^i\partial_i\phi_k|_{\partial\mathcal{M}}$.

In [36, 31] it is show how the spectral data determines uniquely the manifold $\mathcal{M}$, the metric g and the variable mass V. It is shown that the boundary spectral data determines

the set of boundary distance functions. As we have shown in the previous paragraph this also defines the metric.

To obtain these data from a boundary CFT, we need additional assumptions, either on the bulk manifold or on the analytic structure of the CFT. For instance, if the space-time manifold has a time-like global Killing vector, then we can reinterpret $\mathcal{M}$ as its constant-time section. Then the eigenvalues λ_k are determined by the conformal weights of the CFT [11].

For a generic bulk manifold, this interpretation is not possible. Nevertheless, spectral boundary data can be obtained if the two-point correlator of CFT operators of arbitrary dimension Δ, $F(\Delta, x, y) \equiv \langle O^\Delta(x) O^\Delta(y)\rangle$, is a known *analytic* function of Δ. In this case, the poles of this function determine the λ_k. Of course, analyticity in Δ is a rather tall order on a generic CFT!

5 Summary, Conclusions, Speculations

In Section 3 we found that the Euclidean geon is in some cases non-rigid, yet its metric can be determined if we know all its boundary geodesics, not only the minimizing (shortest) ones. Indeed, in all examples we gave, manifest non-rigidity was associated to the existence of a region unreachable by *shortest* geodesics. That limitation was crucial. Longer geodesics, with nonzero winding number, can reach all points inside all spaces studied in Section 3. So, neither the AdS_3 point particle at finite temperature, nor its $t = 0$ section, nor the small ($r_+ \ll 1$) geon possess regions that cannot be reached by some geodesic. If one can find an unambiguous way to determine the length of non-minimal geodesics from boundary data, then these spaces may be boundary rigid after all. They all share one common property: they are quotients by discrete isometries of a boundary rigid space: AdS_3. This leads us to the following conjecture:

> *Quotients of boundary rigid manifolds by discrete isometries are also boundary rigid if they have the same scattering relation.*

In stating the conjecture, we used the fact that the natural way to obtain the spectrum of *all* boundary geodesics is through the scattering relation.

If true, this conjecture would give a concrete, computationally effective way to reconstruct a bulk metric from simple holographic data.

So, it is important to see if the scattering relation can be determined by the CFT correlators. As we saw in Subsection 4.2, the "physical" way of obtaining it is only approximate. To do better, we must assume some additional analyticity property in Δ for the two-point correlators of the CFT. Specifically, if $F(\Delta, x, y)$, defined in the previous

subsection, is analytic for $\Delta \gg 1$, then one can us the geodesic approximation to arrive at

$$F(\Delta, x, y) = \sum_i \text{const}_i \left\{1 + O[L/\Delta D_i(x,y)]\right\} \exp[-\Delta D_i(x,y)/L]. \tag{48}$$

Here the sum extends to *all* geodesics between the boundary points x and y. Since $F(\Delta, x, y)$ is analytic in Δ, its inverse Laplace transform, $\tilde{F}(t, x, y)$ contains delta functions located precisely at $t = \Delta_i(x, y)$

$$\tilde{F}(t, x, y) = \sum_i \text{const}_i \, \delta[t - \Delta_i(x, y)] + ... \tag{49}$$

The ellipsis denote less singular terms.

Finally, we must remember that in the case when the CFT is a gauge theory, there are additional non-local observables with a simple geometric interpretation in the holographic dual. One such observable is the Wilson loop. In particular, the correlator of two Wilson loops is $\propto \exp(-S_m)$, where S_m is the minimal surface between the two loops [37]. This leads to another inverse problem; namely: when is it possible to reconstruct the metric of a manifold with a known spectrum of minimal surfaces in between boundary loops?

Acknowledgments

We would like to thank D. Berenstein, M. Kleban, J. Maldacena, and especially G. Uhlmann for helpful discussions. The work of M.P. is supported in part by NSF through grants PHY-0070787 and PHY-0245068. R.R. is supported by DOE under grant DE-FG02-90ER40542.

References

[1] G. 't Hooft, arXiv:gr-qc/9310026; L. Susskind, J. Math. Phys. **36**, 6377 (1995) [arXiv:hep-th/9409089].

[2] R. Bousso, Class. Quant. Grav. **17**, 997 (2000) [arXiv:hep-th/9911002].

[3] J. M. Maldacena, Adv. Theor. Math. Phys. **2**, 231 (1998) [Int. J. Theor. Phys. **38**, 1113 (1999)] [arXiv:hep-th/9711200].

[4] O. Aharony, S. S. Gubser, J. M. Maldacena, H. Ooguri and Y. Oz, Phys. Rept. **323**, 183 (2000) [arXiv:hep-th/9905111].

[5] L. Susskind and N. Toumbas, Phys. Rev. D **61**, 044001 (2000) [arXiv:hep-th/9909013]; S. B. Giddings and M. Lippert, Phys. Rev. D **65**,

024006 (2002) [arXiv:hep-th/0103231]; B. Freivogel, S. B. Giddings and M. Lippert, Phys. Rev. D **66**, 106002 (2002) [arXiv:hep-th/0207083].

[6] P. Kraus, H. Ooguri and S. Shenker, Phys. Rev. D **67**, 124022 (2003) [arXiv:hep-th/0212277]; T. S. Levi and S. F. Ross, Phys. Rev. D **68**, 044005 (2003) [arXiv:hep-th/0304150]; L. Fidkowski, V. Hubeny, M. Kleban and S. Shenker, arXiv:hep-th/0306170.

[7] V. Balasubramanian and S. F. Ross, Phys. Rev. D **61**, 044007 (2000) [arXiv:hep-th/9906226].

[8] M. Banados, C. Teitelboim and J. Zanelli, Phys. Rev. Lett. **69**, 1849 (1992) [arXiv:hep-th/9204099];
M. Banados, M. Henneaux, C. Teitelboim and J. Zanelli, Phys. Rev. D **48**, 1506 (1993) [arXiv:gr-qc/9302012].

[9] J. Louko and D. Marolf, Phys. Rev. D **59**, 066002 (1999) [arXiv:hep-th/9808081];
J. Louko, D. Marolf and S. F. Ross, Phys. Rev. D **62**, 044041 (2000) [arXiv:hep-th/0002111].

[10] S. S. Gubser, I. R. Klebanov and A. M. Polyakov, Phys. Lett. B **428**, 105 (1998) [arXiv:hep-th/9802109]

[11] E. Witten, Adv. Theor. Math. Phys. **2**, 253 (1998) [arXiv:hep-th/9802150].

[12] M. Henningson and K. Skenderis, JHEP **9807**, 023 (1998) [arXiv:hep-th/9806087].

[13] S. de Haro, S. N. Solodukhin and K. Skenderis, Commun. Math. Phys. **217**, 595 (2001) [arXiv:hep-th/0002230].

[14] C. B. Croke, *Rigidity Theorems in Riemannian geometry*,
http://www.math.upenn.edu∼ccroke/papers.html.

[15] R. Michel, Invent. Math. **65**, 71 (1981).

[16] C. B. Croke, J. Diff. Geom. **33**, 445 (1991).

[17] L. Pestov and A. Sharafutdinov, Sibirskii Math. Zhurnal **29**, 114 (1988).

[18] V. A. Sharafutdinov, Siberian Math. J. **33** 533 (1993).

[19] M. Lassas, V. Sharafutdinov, G. Uhlmann, Math. Ann. **325**, 767 (2003).

[20] C. B. Croke, N. S. Dairbekov, V. A. Sharafutdinov, Trans. Amer. Math. Soc. **352**, 3937 (2000).

[21] L. Pestov, G. Uhlmann, *The Boundary Distance Function and the Dirichlet-to-Neumann map,* (private communication).

[22] C. B. Croke, Comment. Math. Helv. **65**, 150 (1990).

[23] M. Gromov, J. Differential Geom. **18**, 1 (1983).

[24] G. Besson, G. Courtois, S. Gallot, Ergodic Theory Dynam. Systems **16**, 623 (1996).

[25] L. Andersson, M. Dahl, R. Howard, Trans. Amer. Math. Soc. **348**, 2307 (1996).

[26] A.P. Calderon, *Seminar on Numerial Analysis and its Applications to Continuum Physics*, Soc. Brasileira de Matematica, Rio de Janeiro (1980), 65.

[27] J. Lee, G. Uhlmann, Comm. Pure Appl. Math. **42**, 1097 (1989).

[28] M. Lassas, G. Uhlmann, Ann. Sci. cole Norm. Sup. **4** 34, no. 5, 771 (2001).

[29] M. Lassas, M. Taylor, G. Uhlmann, Comm. in Analysis and Geometry, **19**, 207 (2003).

[30] G. Uhlmann, On the Local Dirichlet-to-Neumann Map, to appear in Springer-Verlag, Lecture Notes in Mathematics.

[31] A. Katchalov, Y. Kurylev, M. Lassas, *Inverse boundary spectral problems*, Chapman and Hall, Monographs and Surveys in Pure and Applied Mathematics 123 (2001).

[32] S. Hemming, E. Keski-Vakkuri and P. Kraus, JHEP **0210**, 006 (2002) [arXiv:hep-th/0208003].

[33] V. Balasubramanian, P. Kraus, A. E. Lawrence and S. P. Trivedi, Phys. Rev. D **59**, 104021 (1999) [arXiv:hep-th/9808017].

[34] M. Bianchi, M. B. Green, S. Kovacs and G. Rossi, JHEP **9808**, 013 (1998) [arXiv:hep-th/9807033].

[35] S. W. Hawking and D. N. Page, Commun. Math. Phys. **87**, 577 (1983).

[36] M.I. Belishev, Y.V. Kurylev, Comm. PDE **17**, 767 (1992).

[37] S. J. Rey and J. T. Yee, Eur. Phys. J. C **22**, 379 (2001) [arXiv:hep-th/9803001]
J. M. Maldacena, Phys. Rev. Lett. **80**, 4859 (1998) [arXiv:hep-th/9803002].
S. J. Rey, S. Theisen and J. T. Yee, Nucl. Phys. B **527**, 171 (1998) [arXiv:hep-th/9803135]
D. Berenstein, R. Corrado, W. Fischler and J. M. Maldacena, Phys. Rev. D **59**,

105023 (1999) [arXiv:hep-th/9809188]
N. Drukker, D. J. Gross and H. Ooguri, Phys. Rev. D **60**, 125006 (1999) [arXiv:hep-th/9904191].